JOURNAL OF GEOPHYSICAL RESEARCH, VOL. 87, NO. A3, PAGES 1383–1394, MARCH 1, 1982

Titan's Ion Exosphere Observed From Voyager 1

R. E. HARTLE

Laboratory for Planetary Atmospheres, NASA Goddard Space Flight Center, Greenbelt, Maryland 20771

E. C. SITTLER, JR., K. W. OGILVIE, AND J. D. SCUDDER

Laboratory for Extraterrestrial Physics, NASA Goddard Space Flight Center, Greenbelt, Maryland 20771

A. J. LAZARUS

Center for Space Research, Massachusetts Institute of Technology, Cambridge, Massachusetts 02139

S. K. ATREYA

Space Physics Research Laboratory, University of Michigan, Ann Arbor, Michigan 48105

Electron and ion measurements made by the Voyager 1 plasma science instrument revealed a plasma wake surrounding Titan in Saturn's rotating magnetosphere. This wake is characterized by a plasma that is more dense and cooler than the surrounding subsonic magnetospheric plasma. The density enhancement is produced by the deflection of magnetospheric plasma around Titan and the addition of exospheric ions picked up by the rotating magnetosphere. By using simple models for ion pickup in the ion exosphere outside Titan's magnetic tail and ion flow within the boundaries of the tail, the interaction between Saturn's rotating magnetosphere and Titan is shown to resemble the interaction between the solar wind and Venus. Outside the magnetic tail of Titan, pickup of H^+ formed by ionization of the H exosphere is indicated when synthetic and observed ion spectra are matched. Close to the boundary of the tail, a reduction in plasma flow speed is found, providing evidence for mass loading by the addition of N_2^+/H_2CN^+ and N^+ to the flowing plasma. The boundary of the tail is indicated by a sharp reduction in the flux of high-energy electrons, which are removed by inelastic scattering with the atmosphere and centrifugal drift produced when the electrons traverse the magnetic field draped around Titan. Within the tail the plasma is structured as the result of spatial and/or temporal variations. The ion mass cannot be determined uniquely in the tail; however, one measurement suggests the presence of a heavy ion with a mass of order 28 amu: One candidate is H_2CN^+, suggested as the dominant topside ion of the ionosphere, which may flow from the ionosphere into the tail.

INTRODUCTION

Since the discovery of CH_4 on Titan by *Kuiper* [1944], this satellite has been known to possess a substantial atmosphere. One of the main objectives of the Voyager 1 mission at Saturn was to fly close to Titan so that studies of its atmosphere, ionosphere, magnetic field, and interaction with Saturn's rotating magnetosphere or solar wind could be performed. Measurements by the radio science instrument [*Tyler et al.*, 1981], the infrared spectrometer [*Hanel et al.*, 1981], and the extreme ultraviolet spectrometer [*Broadfoot et al.*, 1981] combined to reveal a dense atmosphere dominated by N_2, as predicted earlier by *Hunten* [1977] and *Atreya et al.* [1978]. The atmosphere was found to be highly extended, having an exobase about 1430 km from the surface (Titan's radius is 2575 km; G. L. Tyler, private communication, 1981) where N_2 and H were observed in significant quantities [*Broadfoot et al.*, 1981]. Although sometimes Titan must be in the solar wind, during the Saturn encounter period, it was observed to be situated within the magnetosphere of Saturn by the plasma science experiment [*Bridge et al.*, 1981], the magnetometer [*Ness et al.*, 1981], and the plasma wave experiment [*Gurnett et al.*, 1981]. The rotating magnetospheric plasma was found to be in a subsonic state [*Bridge et al.*, 1981] as it was deflected around Titan, and it formed a wake region through which the spacecraft passed. The magnetic field measurements [*Ness et al.*, 1981] revealed that Titan does not have an intrinsic magnetic field; however, it was found to possess an induced magnetosphere with a bipolar tail stretching out into the wake region.

A preliminary analysis [*Bridge et al.*, 1981] of the electron and ion energy distribution observed in the wake region indicated that Titan's atmosphere was a significant source of ions for the outer magnetosphere. The main source regions for the ions appeared to be (1) just outside Titan's magnetic tail, where exospheric ions are picked up by the rotating magnetospheric plasma, and (2) within the tail, where ions flow away from Titan. Some of the ions from these sources become a part of Saturn's magnetosphere, while others presumably escape down its magnetotail. The objective of this paper is to make a quantitative interpretation of some 20 measurements of the ion and electron energy distributions that were obtained during the Titan encounter by the plasma science instrument. This interpretation is based partly on comparisons of the measured ion spectra with the synthetic spectra representing models for either ions picked up outside the magnetic tail or ions flowing within the magnetic tail. While the small data set is not sufficient to yield a unique intertpretation, the analysis allows many details of the processes involved in the interaction of the magnetosphere

Paper number 1A1544.

TABLE 1. Measurement Sequence

Type	Measurement time, s	Time to next mode, s
M, high-resolution ions	30.7; 128 steps, 0.24 s per step	6.7
E_1, 10–140-eV electrons	3.84; 16 steps, 0.24 s per step	20.2
L, low-resolution ions	3.84; 16 steps, 0.24 s per step	20.2
E_2, 140–5950-eV electrons	3.84; 16 steps, 0.24 s per step	6.7
Total time = 96*		

*Two such measurement sequences are required to transmit all 128 channels of the M mode; all channels are measured in a given period, but only the upper or lower 72 are telemetered in a given cycle.

with Titan's atmosphere to be elucidated, including the pickup processes in the ion exosphere.

2. Experimental Approach

Instrumentation

The Voyager plasma instrument consists of four potential-modulated Faraday cups (see *Bridge et al.* [1977] for complete description of instrument): three (A, B, C) arranged as a triad equally disposed about an axis pointing in the earthward (nearly solar) direction, supplemented by a single cup (D) whose cone of sensitivity has its axis almost perpendicular to that of the triad. The D-cup axis points approximately in the direction of corotational flow in Saturn's magnetosphere [*Bridge et al.*, 1981]. All four cups make both high- and low-resolution measurements of the ion velocity distribution functions; the D cup measures ion and electron distribution functions alternately. Various sequences of measurements are used at various stages of the mission; during the encounter with Titan the sequence used is described in Table 1. The energy/charge range for ions is from 10 to 5950 eV/Q, and the high (M mode) and low (L mode) nominal resolutions are $\Delta E/E \simeq 3.6\%$ and 29%, respectively. The same energy range for electrons is broken into the E_1 mode from 10 to 140 eV (with $\Delta E/E \simeq 9.9\%$) and the E_2 mode from 140 to 5950 eV (with $\Delta E/E \simeq 29\%$).

Spacecraft Trajectory, Coordinate System, and Cup Orientation.

During the encounter, the spacecraft moved at 17.3 km s^{-1} with respect to Titan, along a trajectory illustrated in Figure 1. In the 96 s separating successive observation cycles the spacecraft moved a distance of 1660 km, or 0.63 Titan radii. The point of closest approach to Titan was situated just behind the dusk terminator, and the distance of the spacecraft from Titan's center was 6969 km at 0540:20 UT (spacecraft event time, SCET). The Titan-centered coordinate system used in Figure 1 has the y axis directed toward Saturn, the x axis directed downstream in the corotational direction, and the z axis parallel to Saturn's rotation axis. Figure 1 shows the trajectory projected onto the xy plane; the trajectory is inclined at approximately 10° to the xy plane, starting out above it and crossing it at 0542 UT. Figure 1 also indicates by circled numbers the positions of the spacecraft at times when crucial ion measurements were made and shows unit vectors pointing in the viewing direction of all four cups at Titan encounter. Each of the cups has appreciable sensitivity over wide angles centered about the direction of the corresponding unit vectors. Thus, for example, the D cup points in a direction close enough to the corotation direction to be fully sensitive to ions from that direction, whereas the other three cups have only partial sensitivity to such ions. Electrons, being very subsonic, can be detected independently of their flow direction.

Electron Feed-Through Corrections.

The observed ion distributions are corrected for electron feed-through contamination, which becomes important for ion fluxes observed near the instrument noise level. Electron feed-through [*Vasyliunus*, 1971] is produced by suprathermal electrons such as those observed within Saturn's outer magnetosphere [*Sittler et al.*, 1981]. It is a result of changes in the electron trajectories when the voltage applied to the modulator grid is switched between its lower and upper levels at the synchronous detection frequency to define a particular energy per charge channel. These trajectory changes cause those electrons intersecting the collector plate

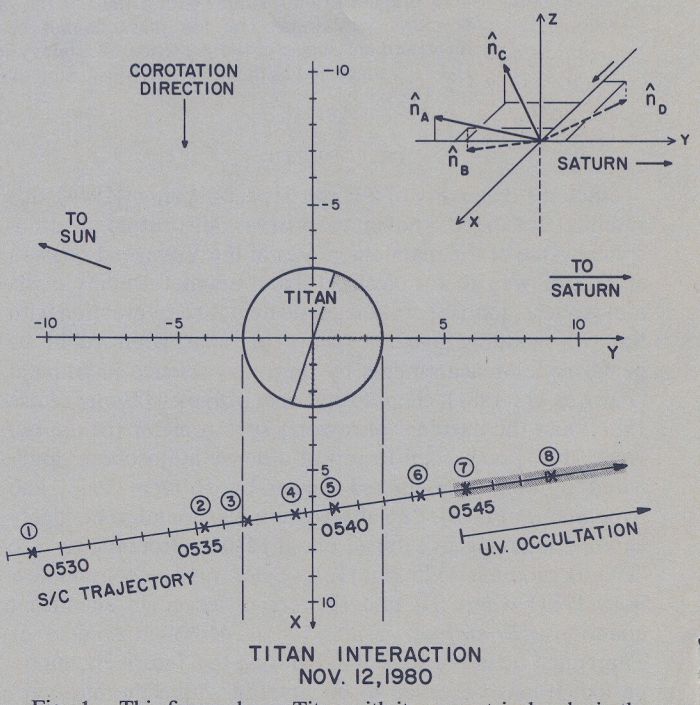

Fig. 1. This figure shows Titan with its geometrical wake in the corotational direction and the encounter trajectory projected onto Titan's orbital plane (x, y). Interval spacings on the x and y axes are in units of 10^3 km. The points marked with numbers represent the spacecraft locations where ion measurements, which are discussed in the text, were taken. The trajectory is inclined to the xy plane at an angle of approximately 10°, crossing it from above to below at 0542 UT. The inset in the upper right shows the directions of the unit normals to the four cups, A, B, C, and D.

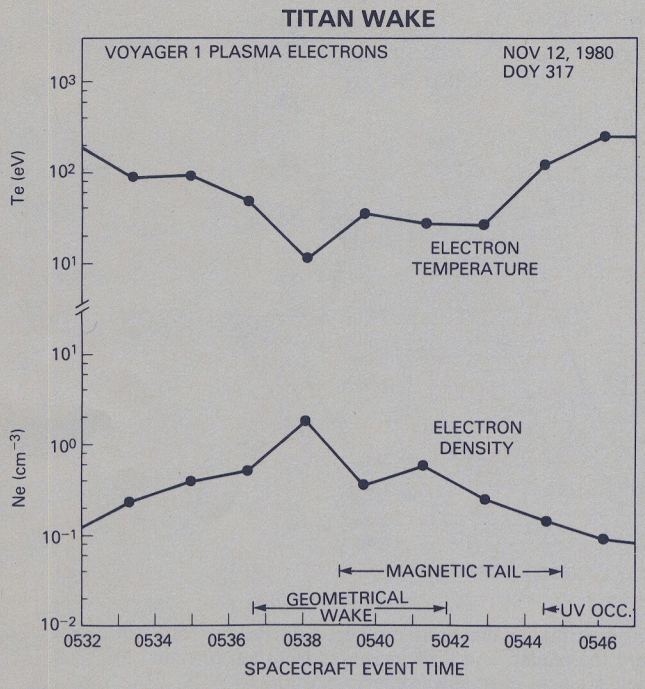

Fig. 2. Electron temperature and density measurements made during the crossing of Titan's wake. These are calculated by taking moments of the measured distribution functions. The density points have been joined by straight lines.

near its edge alternately to hit or miss it, resulting in a small but nonnegligible square wave current that is in phase with the positive ion current, thus increasing that current. The feed-through current can be simulated with a program used to generate synthetic ion distributions (described below), except that electrons instead of ions are fed into the instrument when it is in its positive ion mode. The suprathermal electrons observed near Titan can be approximated for these purposes with a Maxwellian distribution of density and temperature equal to 0.01 cm^{-3} and 1 keV, respectively. Using this model, we computed the electron feed-through, which was then subtracted from the observed ion fluxes before analysis.

Analysis

In order to interpret the interaction between Saturn's magnetospheric plasma and the atmosphere of Titan, we use both ion and electron measurements. The electron densities and temperatures are computed by taking moments of the distribution function deduced from the electron measurements, using the analysis procedures outlined in *Scudder et al.* [1981]. When the spacecraft is in full sunlight this analysis yields reliable determinations of these fluid parameters, and complications of composition and dependence of the instrument response upon the Mach number of the flow do not apply.

When the flow is transonic, as was generally found near Titan, ion fluxes are simultaneously observed in all four cups, resulting in a complicated (though well-understood) convolution of the instrument response function and the ion distribution function. The ion analysis does not yield a model-free interpretation of the ion distribution functions in terms of fluid parameters. Instead, using a numerical code (developed by V. M. Vasyliunas) for simulating the convolution of the instrument response and model ion distribution functions, we calculate 'synthetic distributions.' Since more than one ion species may be present, the composition and other appropriate parameters of the model distribution (density, temperature, bulk velocity) are varied, and the synthetic and observed distributions are compared until an optimum match in all four sensors is acquired, thereby yielding estimates of the model dependent parameters.

3. Plasma Observations in Titan's Wake

The first signatures of Titan's wake in Saturn's magnetosphere appeared in the electron and ion spectra at about 10,000 km from Titan's center (or at about 0532 UT) as is evident in the electron densities N_e and temperatures T_e shown in Figure 2. After this time, the electron densities began to increase gradually, while the electron temperatures began to fall as the spacecraft moved into the wake. Between about 0536 and 0538 UT the electron densities increased more rapidly, and a maximum value of 1.8 cm^{-3} was measured at 0538 UT, just outside the magnetic tail. This density value was more than an order of magnitude greater than the background magnetospheric density of about 0.07–0.3 cm^{-3} observed just before entering the wake region. The density buildup described here is interpreted as being due to the addition of electrons and ions which are formed by ionization of Titan's exosphere and then 'picked up' by Saturn's rotating magnetospheric plasma. This model will be discussed in detail in the next section.

As the spacecraft entered the wake region, the electron temperature decreased; during the period between 0536 and 0538 UT, the electron temperature decreased more rapidly, reaching a minimum value at the time of the electron density peak. This minimum measured temperature is approximately 20 times less than the background magnetospheric temperature of about 200 eV. The lower temperatures in the wake were interpreted in *Bridge et al.* [1981] to be the result of the addition of cooler electrons formed by the ionization of the exosphere and the cooling down of the magnetospheric electrons through collisions with Titan's neutral atmosphere.

In lobe L_1 of the magnetospheric tail (as defined by *Ness et al.* [1981]), the electron density was distinctly below the peak value observed just outside the tail and continued to decline in lobe L_2. The electron temperatures rose in this region, exhibiting an increase in lobe L_2. After 0544 UT, the apparent drop in the electron density and increase in the electron temperature occurred when the spacecraft was in the UV occultation region. The ion spectra independently indicated a rise in the plasma density, reaching a value of about 1 cm^{-3} at 0544:59 UT. The apparent drop in the electron density is interpreted as being due to the spacecraft acquiring a negative potential in relation to the surrounding plasma. This is a consequence of the absence of a photoelectron current to the spacecraft when it was in the UV occultation region. When the spacecraft potential went negative those electrons with energies below the potential barrier were not measured, and the calculated electron densities were below the ambient values, which in turn artificially increased the calculated electron temperature.

Another feature of the magnetospheric interaction with Titan is evident in the electron velocity distribution functions observed in the wake region and displayed in Figure 3: An electron depletion or 'bite-out' occurred in the electron

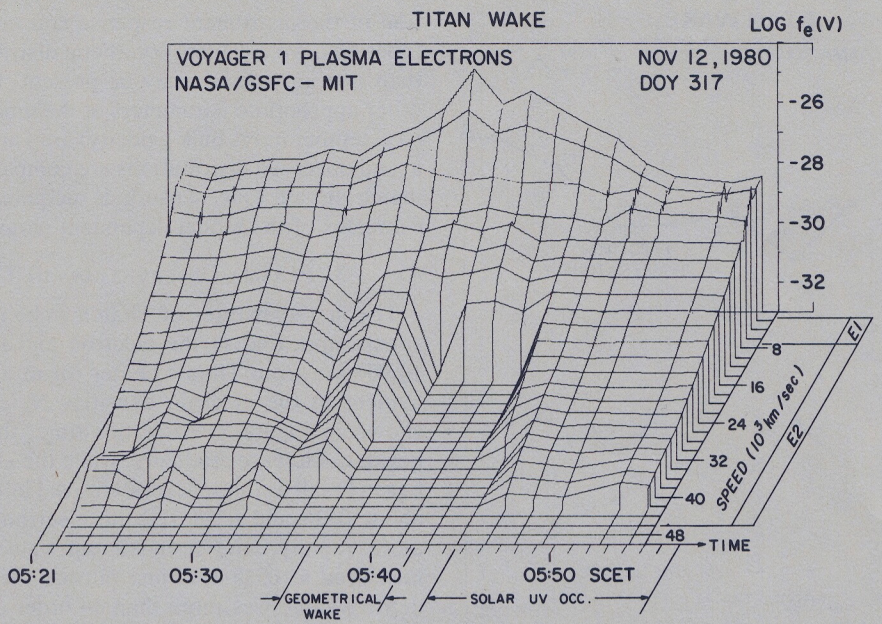

Fig. 3. A three-dimensional representation of the electron distribution functions measured during the 'bite-out' feature. Log f_e (V) is plotted vertically, speed is plotted toward the reader, and time increases from left to right. An individual distribution is plotted at a time corresponding to measurement of its lower-energy portion.

spectra above 700 eV between 0538:45 and 0543:45 UT (note that 48 s have been added to the times shown in Figure 3 to mark the times when the 700 eV measurments were made). The bite-out can be expanded to fill the period between 0537:15 and 0545:15 UT if the electron depletions above 3 keV are included. We note that this overall bite-out region not only includes the entire magnetic tail but also extends just outside its boundaries.

The dynamical properties of the plasma flowing in the wake are embodied in the ion energy distributions measured separately in each Faraday cup A, B, C, and D and shown in Figures 4 and 5. Outside the wake region, ion distributions were observed in all four cups, each measuring rather uniform distributions over a broad energy range, as indicated by the representative observations at points 1 and 8 shown in Figures 4 and 5, respectively. These background magnetospheric ion populations are much hotter than those observed in the inner magnetosphere of Saturn [*Bridge et al.*, 1981], where about half the time the energy distributions have two distinct peaks believed to be produced by H^+ and N^+ (and/or O^+). In contrast, in the absence of clear peaks in the energy distributions outside Titan's wake, the composition of the plasma is not as clearly revealed. However, in section 4 we identify two distinct components in the ion spectra just outside Titan's wake; namely, H^+ and N^+ (or O^+). An investigation of the background distributions and their time

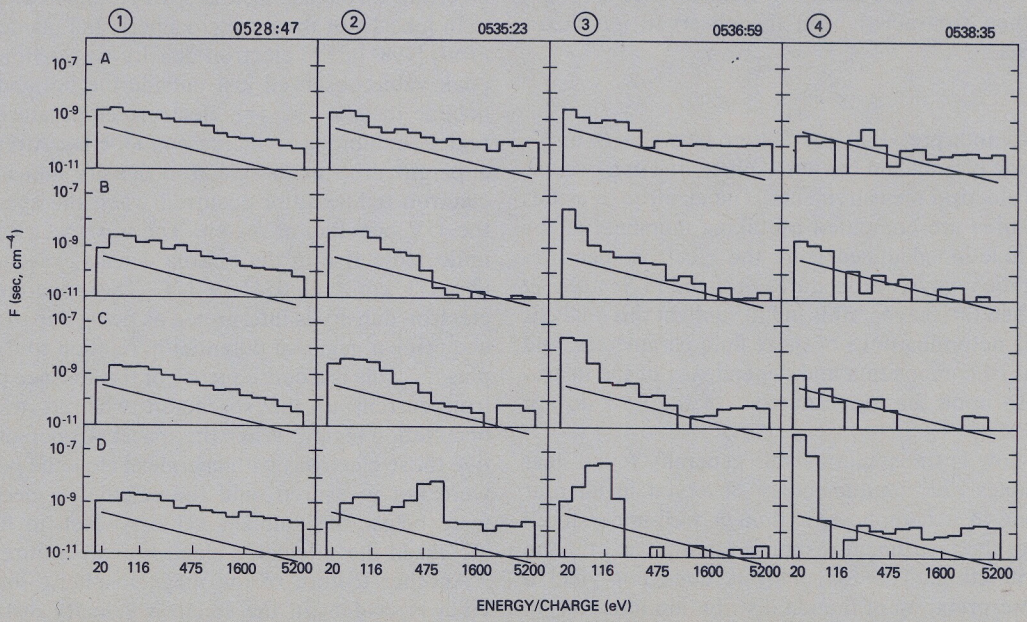

Fig. 4. Distribution functions for ions at the numbered points, Figure 1, on the trajectory plotted vs. energy/charge; A, B, C, and D refer to the sensor cups by which the distributions were measured. The solid slanted lines represent the rms noise level of the instrument. Each distribution, consisting of 16 measurements, requires 3.84 s to complete.

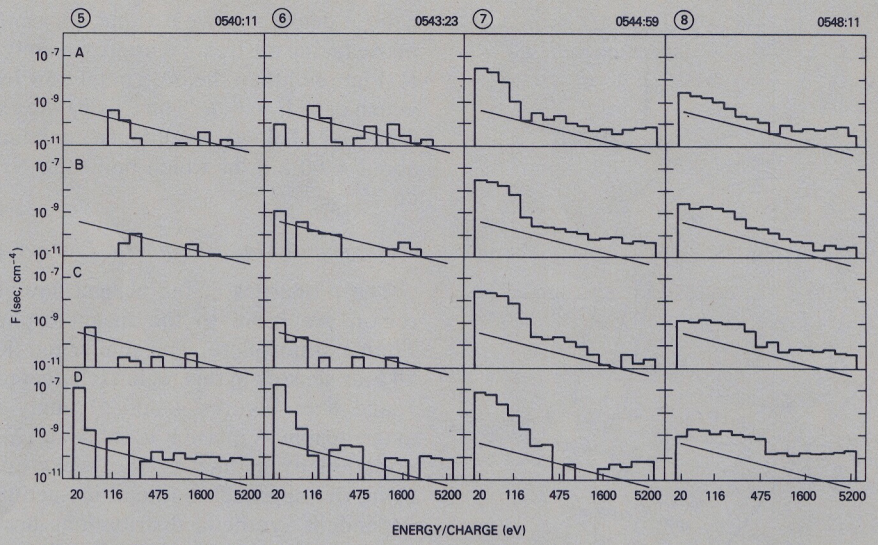

Fig. 5. Similar to Figure 4 for the points 5, 6, 7, and 8 on the trajectory, Figure 1.

variability is carried out by calculating the standard deviation about the mean value of each measurement step for a representative period near the Titan wake. These standard deviations are used as a guide when making comparisons between measured and synthetic distributions which will be described below. Using this procedure, the background ion thermal speeds are estimated to range from 150 to 200 km s^{-1} with flow speeds in the range 80 to 150 km s^{-1}, respectively, corresponding to subsonic flow which is less than the corotational speed of 200 km s^{-1}.

In the outer region of the wake, corresponding to point 2 of Figure 1, the plasma density enhancement shows up as an increase in the amplitude of the ion distribution in the D cup in the mid-energy range, as illustrated in Figure 4. We note that the low-energy peak is within the amplitude range of the background magnetospheric distributions that should be present at point 2. The narrow peak in the mid-energy range indicates that the exospheric ion population added to the flow is cooler than that of the background magnetospheric ions. Small enhancements above the background ion distribution levels appear in the sunward facing cups A, B and C, indicating that the trajectories of the exospheric ions permit them to enter these cups, whose axes make large angles to the presumed flow direction. We show in section 4 that the shapes of the distributions corresponding to the new ions added to the flow are consistent with those expected for ions executing $\mathbf{E} \times \mathbf{B}$ drift motion.

The addition of new ions to the wake becomes more apparent at point 3, where the maximum amplitudes of the ion distributions shown in Figure 4 are about an order of magnitude greater than those at point 2. At point 3 the peaks occur at lower energies, suggesting a combination of a lower effective temperature and drift speed for the drifting ions than at point 2. Finally, the newly born ions attain their lowest observed effective temperature and drift speed at point 4, just outside Titan's magnetospheric tail. This result is displayed in Figure 4, where we note that most of the ions were collected in the D cup, characterizing the presence of cool ion flow.

Cool ion distributions were also observed within lobes L_1 and L_2 of the magnetospheric tail at points 5 and 6, respectively. That is, most of the ion signatures appeared in the low-energy channels of the D cup, as shown in Figure 5. In addition, the high-energy fluxes are considerably reduced from those of Saturn's magnetosphere in the vicinity of Titan. The flow is more likely to be along the magnetic field in the tail than transverse to the field as in the wake outside the tail. This results because the magnetic field is approximately aligned with Titan's tail, while outside the tail the magnetic field is approximately along the z axis. This picture tacitly assumes that an oppositely directed flow toward Titan, which is out of the field of view of the instrument, is not present.

At point 7, well-developed ion energy distributions appearing above those of the background magnetosphere were observed in all four cups, as indicated in Figure 5. Since these distributions decrease with increasing energy in each sensor, the presence of a convective Maxwellian distribution is suggested (described in next section). This observation point differs from the others in that the measurements were made at the outer edge of the magnetic depression that characterizes the outer boundary of tail lobe L_2 [*Ness et al.*, 1981].

4. Discussion

To describe the processes involved in the interaction of Saturn's rotating magnetosphere with Titan's atmosphere and ionosphere, we propose a simple model that is analogous to the interaction of the solar wind with Venus. We illustrate the essential elements of such a model schematically in Figure 6. The analogy we have drawn is based in part on the fact that both Venus [*Russell et al.*, 1980] and Titan [*Ness et al.*, 1981] have weak or no intrinsic magnetic fields. In such a case the magnetized plasma flowing in the vicinity of Titan interacts directly with its atmosphere and ionosphere and produces an induced magnetosphere whose field lines are draped around Titan's ionosphere and stretched out in the wake to form a tail [*Ness et al.*, 1981]. One difference between the interaction at Titan and that at Venus is that the plasma flowing toward Titan is subsonic, while the solar wind flowing toward Venus is supersonic. However, as a consequence of the bow shock at Venus, both plasma flow systems are subsonic when they initially interact with their respective ionospheres.

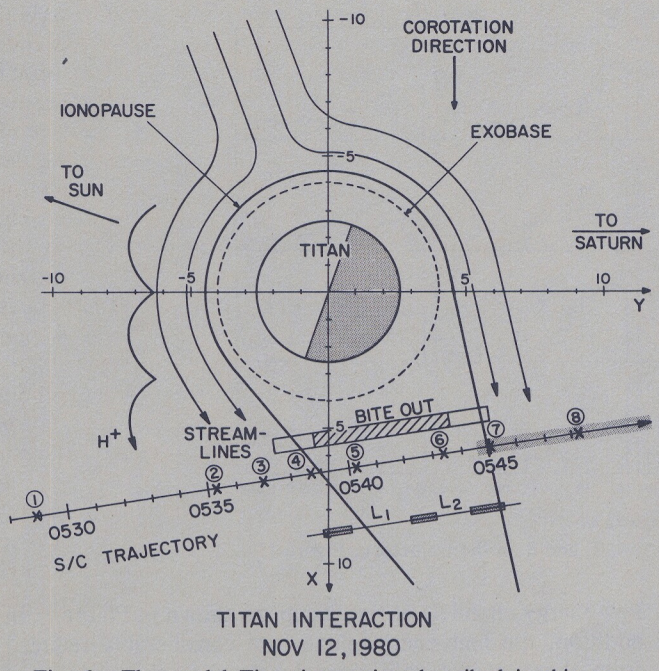

Fig. 6. The model Titan interaction described in this paper. Points on the trajectory are repeated from Figure 1. L_1 and L_2 refer to the lobes of the bipolar magnetic tail, as delineated by the magnetometer measurements [*Ness et al.*, 1981]. The shaded bars refer to regions of local magnetic minima. Incoming flow shows observed 20° deflection from the corotational direction. The trajectory of an H^+ ion is approximately to scale in the measured magnetic field.

One further difference between the interaction of plasma flowing toward Titan and toward Venus results from the fact that the neutral exosphere (principally H and N_2) extends to greater heights above the ionosphere of Titan than that (principally H, He, and O) above the ionosphere of Venus. This is a consequence of the gravitational force at Titan's surface being about 6 times less than that at Venus, while Titan's exospheric temperature is only about a factor of 2 less than that of Venus. Thus the plasma flow at Titan is expected to be modified to a greater extent by its neutral atmosphere than the corresponding flow at Venus, as will become evident in the following. In this regard the interaction of Titan's atmosphere with Saturn's magnetosphere may more closely resemble the interaction of the solar wind with the extended atmosphere of a comet [e.g., *Wallis*, 1973] than with the atmosphere of Venus.

By analogy with the interaction at Venus we assume that the hot, rotating magnetospheric plasma of Saturn and the cool ionospheric plasma of Titan are essentially immiscible and are thus separated at a boundary called an ionopause, which is indicated in Figure 6. At the ionopause the ionosphere is expected to terminate abruptly because the ions formed by ionization of the neutral atmosphere extending above the ionopause will be swept away by the flowing magnetospheric plasma. As with Venus the ionopause is not expected to penetrate to altitudes as low as Titan's neutral exobase, which occurs 4000 km from Titan's center, where the density of the major constituent N_2 is 10^8 cm^{-3} [*Broadfoot et al.*, 1981]. We estimate the minimum height of the ionopause as that altitude where the ion-neutral mean free path $1/\sigma n$ equals the scale length for horizontal flow, where $\sigma = 5 \times 10^{-15}$ cm^2 is the ion-neutral cross section and n is the neutral density. If we assume, for simplicity, that the ionopause facing upstream is approximately spherical with radius R (Figure 6) then the horizontal flow length is of order R, in which case $1/\sigma n \approx R$. Thus, using the exospheric distribution for N_2 (see below), we obtain a minimum ionopause radius of about 4400 km, at which point the N_2 density is 4.5×10^5 cm^{-3}.

Background Magnetospheric Plasma of Saturn

The properties of the plasma flow just outside the wake region are basic to the magnetospheric interaction with Titan's atmosphere. The similar ion flux levels observed in all four sensors in this region (characteristic spectra at points 1 and 8 in Figures 4 and 5) imply that the background magnetospheric plasma is subsonic. We quantify this interpretation by estimating the background fluid parameters, using the approach outlined in section 2, in which model-dependent synthetic distributions are derived for all four cups and compared with the observed distributions. In particular we attempt to match the observed distributions with those synthesized from a convective Maxwellian for the jth constituent

$$f_j = n_{0j}(m_j/2\pi kT)^{3/2} \exp\left[-m_j(\mathbf{V} - \mathbf{V}_0)^2/2kT\right] \qquad (1)$$

where m_j is the jth ion mass, $\mathbf{V}$ its velocity, k is Boltzmann's constant, and n_{0j}, $\mathbf{V}_0$, and T are the local density, convection velocity, and temperature, respectively. Referring to the representative points 1 and 8 in Figures 4 and 5, we see that at least two ion components may be expected. The low-energy one is most likely H^+, while the more energetic component, because of its presence in Titan's atmosphere, may be N^+. The presence of N_2^+ and H_2CN^+ is possible, but it cannot be confirmed or ruled out at this time on the basis of matching synthetic with observed distributions. The latter ion H_2CN^+ is believed to be the dominant terminal ion in the topside ionosphere according to a preliminary model (S. K. Atreya et al., unpublished manuscript, 1981). One of the problems in the interpretation of these spectra is that the signal levels are generally low, so that the spectra generally exhibit appreciable statistical fluctuations. Additionally, the magnetospheric plasma shows considerable variability; therefore, we only give ranges for the fluid parameters, deferring a more detailed analysis to a later paper. The variation of the background magnetospheric plasma in the vicinity of the wake is taken into account by calculating the mean value and variance at each energy step, using a number of spectra from the background region. These results provide the necessary constraints for matching the synthetic distributions with the observed distributions.

By matching synthetic distributions for the H^+ component with the observed distributions we obtain flow velocities approximately aligned along the corotation direction, with flow speeds ranging between 80 to 150 km s^{-1}, considerably below the 200 km s^{-1} expected for corotation. These low rotational velocities are consistent with the subrotation speeds observed elsewhere during the incoming pass through the magnetosphere [*Bridge et al.*, 1981]. These simulations also suggest a slight inward deflection of the flow toward Saturn by about 20° from the corotational direction. If present, this deflection may be due to an inward movement of Saturn's magnetosphere responding to an increasing solar wind ram pressure. Such an increase in the ram

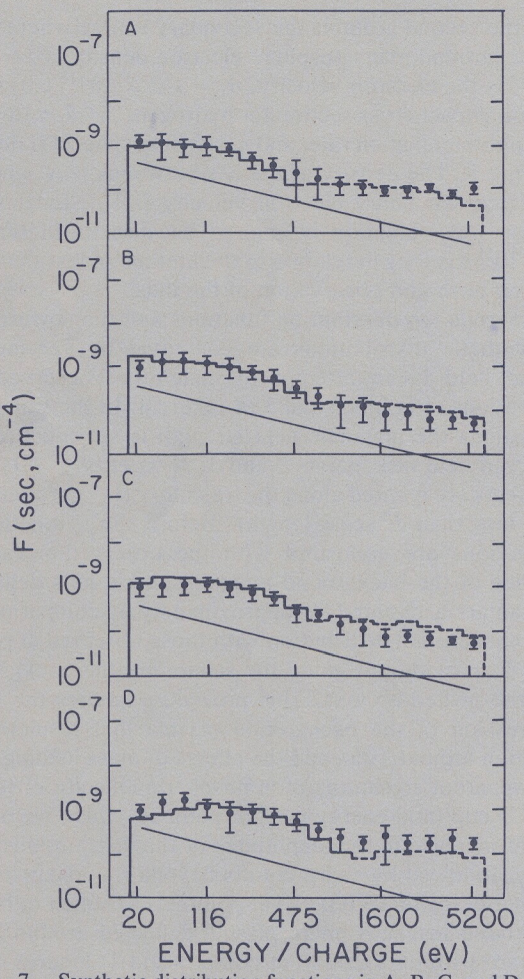

Fig. 7. Synthetic distribution functions in A, B, C, and D sensor cups for the background magnetosphere plasma in the vicinity of Titan, where H^+ (solid line) and N^+ (dashed line) have been used. The data refer to the observed distributions while the eccentric positions of the corresponding error bars result from the logarithmic scale.

pressure during the Titan flyby is predicted by plasma measurements made upstream by Voyager 2 (J. D. Sullivan and P. R. Gazis, private communication, 1980).

The range of the H^+ thermal speed inferred from the matching procedure is 150 to 200 km s^{-1}, corresponding respectively to the flow speeds 80 to 150 km s^{-1}, which are subsonic as noted before. Similar flow velocities and thermal speeds were computed for an N^+ (or O^+) component, indicating that H^+ and N^+ (or O^+) are probably co-moving and that insufficient time has lapsed to exchange their thermal energies to produce thermal equilibrium. In Figure 7 we compare representative synthetic distributions for H^+ and N^+, having flow speeds of 100 km s^{-1}, with the mean values and variances of the ion spectra observed in the vicinity of Titan. A reasonably good match between the synthetic distribution for H^+ and the observed spectra is obtained while small differences occur for the N^+ component. These differences may be reduced by including the possible anisotropies in the velocity distribution and by adding a third component such as N_2^+ or H_2CN^+.

Ion Exosphere

The electron and ion measurements suggest an atmospheric origin for the plasma density buildup observed in the wake on the side of Titan facing away from Saturn. Electrons and ions produced by ionization of the neutral exosphere extending above the ionopause would be picked up and carried downstream in the wake by Saturn's magnetospheric plasma as it is deflected around Titan. Evidence for the presence of such an ion exosphere accrues in part from the fact that the electron and ion temperatures decrease as the plasma density builds up, corresponding to the addition of increasing numbers of cooler exospheric ions and electrons to the hotter magnetospheric plasma. Additional evidence is drawn from the fact that the plasma flow speed also decreases as the plasma density increases. Such a slowing down or mass loading effect [*Michel*, 1971] is expected when low-velocity ions are added in sufficient quantity to the more rapidly flowing magnetospheric plasma. At birth the exospheric ions have velocities and energies (<1 eV) that are much less than those of the magnetospheric plasma.

An atmospheric origin for the plasma buildup, of course, requires a sufficiently dense neutral exosphere to produce enough ions to form the ion exosphere. Atomic hydrogen H and molecular nitrogen N_2 were observed in the exosphere of Titan with concentrations of 4×10^4 cm^{-3} and 10^8 cm^{-3}, respectively, at the exobase [*Broadfoot et al.*, 1981]. According to a preliminary model of the neutral atmosphere and ionosphere (S. K. Atreya et al., unpublished manuscript, 1981), H and N_2 are expected to be the major constituents in the exosphere. Thus we consider the radial density distributions of H and N_2 in the exosphere shown in Figure 8. These distributions were derived from a spherically symmetric exosphere model [*Hartle*, 1971] by using an exospheric temperature of 160°K and a gravitational acceleration of 58 cm s^{-2} at the exobase (137 cm s^{-2} at surface). Although N_2 is almost 4 orders of magnitude more dense than H at the exobase, we see that H quickly becomes the dominant constituent at about 1200 km above the exobase, while decreasing by only an order of magnitude in a distance of about 5000 km. We note that the variations of the wake plasma and H are similar, wherein the electron density varies by about an order of magnitude in 6000 km. Thus because of the great exent of H above the ionopause and its similar variation to that of N_e, atomic hydrogen appears to be the most likely source gas for the plasma enhancement in the outer portion of the wake. We examine this possibility first.

When exospheric ions are newly born in the magnetospheric plasma flowing at velocity $\mathbf{V}_m$, they will be accelerated in the motional electric field $\mathbf{E} = -\mathbf{V}_m \times \mathbf{B}$, where $\mathbf{B}$ is the magnetic field. Since the exospheric ions are born with energies significantly less than the streaming energy of the plasma, they travel in cycloidal trajectories according to their $\mathbf{E} \times \mathbf{B}$ drift motion, indicated in Figure 6 for H^+. To test the hypothesis that the ion enhancements are produced by exospheric ions traveling in cycloidal paths, we construct a simple kinetic model for ion velocity distributions made up of ions with such trajectories. The resulting 'cycloidal ion distributions' are then fed into a numerical code that simulates the plasma instrument and computes synthetic ion distributions for each Faraday cup. The synthesized distributions are then compared with the observed ones.

The cycloidal ion distributions are derived by computing a large number of ion trajectories from their points of birth to the points where they cross the spacecraft trajectory (1000 trajectories per observation point are used). The ion velocity

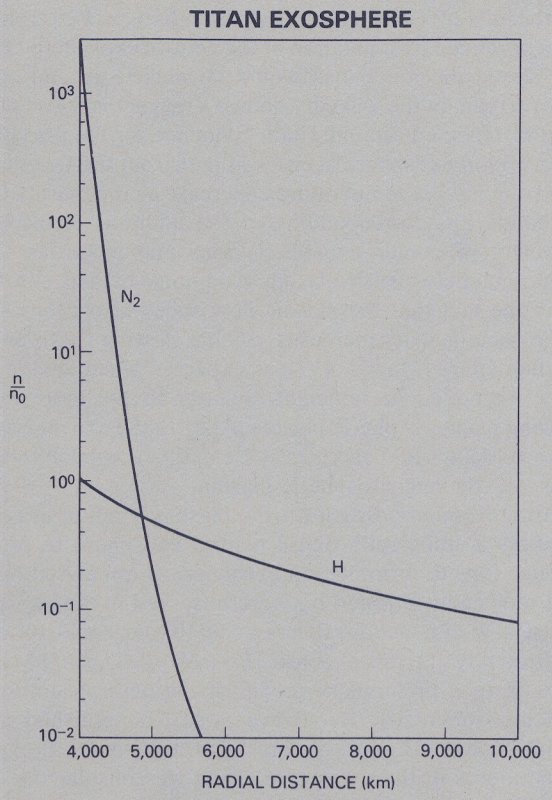

Fig. 8. Normalized radial density profiles for model exosphere of Titan described in text. The normalization constant n_0 is the density of H at the exobase.

distribution functions are then computed at selected observation points by summing up all the particles in each velocity interval. Since the electric and magnetic fields are not known along the ion trajectories through either observations or models, we simplify the ion trajectory computations at this preliminary stage of analysis by choosing a uniform magnetic field pointing in the negative z direction and the one-dimensional electric field $E = E(y')$ pointing in the negative y' direction, where x' and y' are new axes formed when the x and y axes, respectively, are rotated counterclockwise by an angle θ about the z axis. The ion drift velocity $V_D = E/B$ is directed along the positive x' axis, and consequently $E(y')$ decreases as y' decreases, producing the expected reduction in V_D caused by mass loading. To approximate the effects of the expected curved streamlines around Titan, we also examine a few cases having an electric field $E = E_0/r^2$ directed radially away from Titan in the upstream region, where r is the distance from Titan's center. Downstream, the radial field blends into the one-dimensional field of $E(y')$. The resulting ion distributions from this configuration differ little from those derived solely from the one-dimensional electric field. Consequently, the simulation concentrates on distributions computed from the one-dimensional field, leaving the more complex, self-consistent, flow field modeling to studies just underway.

The number of ions emitted from a particular source point in the atmosphere are taken to be proportional to the volume production rate

$$P = (N_e V_e \sigma_1 + J)n + NV_e' \sigma_1 n \qquad (2)$$

where only the important ionization sources are included. The first group of terms is the primary ionization source, while the second group is the secondary source where N_e is the background magnetosphere electron density, $V_e \simeq 9000$ km s^{-1} is the electron velocity, $\sigma_1 = 1\text{–}2 \times 10^{-16}$ cm^2 is the electron impact cross section for hydrogen, $J = 5 \times 10^{-9}$ s^{-1} is the photoionization rate, and n is the exospheric H density of Figure 8. The density of the newborn ions is N, and the associated secondary electron velocity is V_e'. Ion loss by electron recombination is ignored because its lifetime of about 10^{11} s is long in relation to the lifetime of less than 50 s between birth and observation of the ions.

Numerous ion distribution functions and the corresponding synthetic distributions are computed by varying the electric field is an attempt to match the observed ion distributions at points 2 and 3 of Figure 4. In the trajectory calculations the magnetic field strength is set equal to 5 γ (observed field near points 2 and 3; *Ness et al.* [1981]) and ∇E effects are ignored along the trajectory (H^+ gyroradius is much less than E scale length). Before the synthetic ion distributions are compared with the observed ones, the presence of the background magnetospheric ions deflected by Titan are accounted for approximately by comparing the mean background distribution with those observed at points 2 and 3, providing a guide for separating the background from the picked-up ions. This procedure ignores the small compression of the background plasma that results from deflection around Titan and the effects of mass loading. The most apparent signatures of atmospheric ions are observed in the D cup (mid-energy peak at point 2), where we note a gradual increase in the amplitudes of the distributions with energy, followed by sharp cutoffs beyond the maxima. The low-energy region ($\lesssim$100 eV) at point 2 is assumed to be the background magnetosphere plasma deflected around Titan (compare with background at points 1 and 8, Figures 4 and 5).

The cycloidal ion velocity distributions are similar in form to elliptically shaped doughnuts whose major and minor axes are in the V_x-V_y plane. The shapes of the distribution functions are not strongly dependent on the magnitude of V_D, in which case the maxima of the distributions in the V_x-V_y plane occur near $(V_x, V_y) \simeq (2\ V_D, 0)$ while the local maxima have amplitudes approximately in the ratio 2:1:0.2 for $V_x/V_y = \infty$:1:0. On the other hand the shapes of the synthetic ion distributions are very sensitive functions of the drift speed. A good match of the synthetic H^+ distributions to the observed distributions at points 2 and 3 results when the drift speeds are 175 km s^{-1} and 85 km s^{-1}, respectively. With this knowledge it is interesting to note that the drift speeds can be quickly estimated by considering the fact that the velocities at the sharp cutoffs correspond approximately to the maximum velocities of ions in cycloidal trajectories, that is 2 V_D.

For completeness we consider the possibility that the ion enhancements at points 2 and 3 may be produced by heavier ions such as N^+ and N_2^+/H_2CN^+. This is done by following the above procedure for calculating cycloidal ion distributions. In this case the derived distributions approximate narrow beams as a result of large gyroradii of about the size of the interaction region. Furthermore, the corresponding densities are considerably smaller than the observed electron densities. Consequently, the simulations cannot be made to match the observed distributions, thereby ruling out the possibility that the ion enhancements are produced by heavy ions formed from the atmosphere of Titan.

As a further check on the analysis we attempt to match the observed distributions with those synthesized from a convective Maxwellian. This distribution leads to good matches with the observations; however, the corresponding ion densities and/or drift speeds are too large at point 2, while they are consistent with the measurements at point 3. In particular, for H^+ at point 2 we require a drift speed of about 400 km s^{-1} to produce a good match. Since this drift speed exceeds the maximum background drift speed of 150 km s^{-1}, we rule out the possibility that the picked-up ions are in a convective Maxwellian distribution at point 2. At point 3 the model density for H^+ is about 0.6 cm^{-3} and the bulk velocity is about 150 km s^{-1}, which are both within the measured constraints (electron density and rotational speed) of the system. Since we can also match the observations at point 3 with cycloidal distributions, this latter example illustrates a lack of uniqueness in our ability to identify the distribution function at point 3.

A rough estimate for the concentration of exospheric H required to produce the plasma density enhancement is made in an explicit manner by considering the charge conservation equation

$$\nabla \cdot N\mathbf{V} = P \tag{3}$$

where $\mathbf{V}$ is the drift velocity of the newly born ions, P is the ion production rate given by (2), and the ion loss rate is neglected because of the long electron recombination time noted previously. The macroscopic approximation (3) is valid because the H^+ gyroradius is considerably less than the H exospheric scale height. Equation (3) is integrated along a streamline by replacing the divergence term with $\partial(NV)/\partial l$, where l is the arc length along a streamline and the cross-sectional area of a stream tube is assumed constant. Thus we obtain

$$\frac{V}{V_e'\sigma_1} \ln\left[1 + \frac{V_e'\sigma_1 N(l)}{N_e V_e \sigma_1 + J}\right] = \int_0^l n dl \tag{4}$$

In the absence of a detailed description of the dynamical properties of the interaction, we treat the background plasma parameters and the drift velocities as constants representing typical values along a streamline. Furthermore, we assume a simple form for the configuration of a streamline, that is, one similar to that shown in Figure 6 that corresponds to Titan-centered spherical shells of radius R in the upstream region. In this case the density integral in (4) is approximately 2 $Rn(R)$. It is interesting to note the small difference between the density integral for the curved streamline and $\sqrt{2}\ \pi RH\ n(R)$, which corresponds to the limiting case of a straight streamline in the x direction, e.g., their ratio 2 $R/\sqrt{2}\ \pi RH$ is in the range of 1.3 to 1.4. By considering background electron and ion densities in the range 0.1–0.3 cm^{-3} (upper value represents the possible compression along streamline) and using the inferred ion drift speeds, we obtain the range 3.5×10^4–2.5×10^5 cm^{-3} for the H exobase densities required to produce the observed density enhancement in the wake. We note that this preliminary estimate is in reasonable agreement with the observed exobase density of 4×10^4 cm^{-3} [*Broadfoot et al.*, 1981]. Furthermore, our upper limit could be reduced if drift speeds upstream are reduced below those at the observation points as is expected in flow around a blunt object.

We examine the narrow ion distributions at point 4, Figure 4, separately from those at points 2 and 3 because they differ in several ways. First, the magnetic field is inclined to the xy plane [*Ness et al.*, 1981] so that the ion drift plane is tilted out of this plane. In this case, some of the ion flux measured in the D cup may have a velocity component along the magnetic field. Second, because of the limited information resulting from measurements in only two energy channels (D cup), we cannot distinguish between cycloidal distributions and convective Maxwellians. Furthermore, the ion composition cannot be resolved at this point because of the limitations in the energy distributions and the absence of a time-coincident electron density measurement. Thus, in addition to H^+, significant contributions from N^+ and N_2^+ are quite possible since the corresponding streamlines in this region, close to the magnetic tail, may pass through regions upstream where the N_2 density is significant. Furthermore, the dominant ion H_2CN^+ predicted for the topside ionosphere (S. K. Atreya et al., unpublished manuscript, 1981) may also be present if it diffuses across the ionopause. If we consider convective Maxwellian ion distributions, good matches of the synthetic ion distributions to the observed distributions are obtained for H^+, N^+, and N_2^+/H_2CN^+ when the bulk speeds are 60, 10, and 5 km s^{-1}; the densities are 2.5, 15, and 30 cm^{-3}, respectively; and the ion temperature is 2.1 eV. Although these densities are higher than the peak electron density we observed at an earlier time, they are compatible with the higher densities inferred from the plasma wave experiment [*Gurnett et al.*, 1981] in this region.

The measurements at point 4 show the first clear evidence for the slowing down of plasma flow by mass addition. In contrast, significant slowing down appears not to have occurred at points 2 and 3 because the drift velocities inferred at these points are within the velocity range of the background magnetosphere plasma. This is consistent with our theoretical estimates for slowing down by the addition of exospheric H^+ at these points. Similarly, we expect little slowing down by H^+ at point 4, suggesting the presence of significant mass loading by the addition of the heavier ions N_2^+/H_2CN^+ and N^+. Furthermore, we find an insufficient quantity of neutral H to produce the inferred ion densities (using the above procedure), showing that self consistency requires the presence of N_2^+/H_2CN^+ and N^+ at point 4.

Since the gyroradius of N_2^+ is considerably larger than the scale height of N_2, a kinetic treatment is required to accurately determine the effect of mass loading by N_2^+. However, we can get an order of magnitude estimate of the importance of mass addition by comparing terms in the momentum equation. That is, we compare the inertial term $\rho V \partial V/\partial s$ in the momentum equation with the force term $-2mVKn$ caused by the pickup of ions [*Hartle et al.*, 1980], where s is the arc length along a stream line, ρ is the ion mass density, V is the ion velocity, m is the N_2^+ mass, and $n \simeq 4 \times 10^5$ cm^{-3} is the N_2 density near the ionopause. The ionization rate $K \simeq 1.3 \times 10^{-8}$ s^{-1} is the sum of the N_2 photoionization rate 5×10^{-9} s^{-1} and the electron impact ionization rate of about 7.5×10^{-9} s^{-1} that results from the background magnetospheric electrons. We approximate the velocity gradient $\partial V/\partial s$ by $V/2R$ where R is the radial distance from Titan's center to the streamline, and $2R \simeq 9 \times 10^8$ cm is taken as the e folding length for the velocity. Since the ion mass density quickly approaches that for N_2^+ in a few hundred kilometers ($\ll R$) along a streamline, then $\rho \simeq mN$ over most of the streamline, where N is the N_2^+ density.

Thus the ratio $f \equiv 2mVKn/\rho V\partial V/\partial s \simeq 4KnR/NV$. The velocity V can range from its upstream value of 80–150 km s^{-1} to the final value of 11 km s^{-1} inferred from the Maxwellian match while the density N can vary from an upstream value of about 0.1 cm^{-3} to a maximum value of 13 cm^{-3}. Considering the initial stages when the density is still low, say 1 cm^{-3}, and the velocity is still high, say 50 km s^{-1} then $f \simeq 2$, indicating that the force caused by mass loading by N_2^+ should be significant in slowing down the plasma. We note that the ratio f remains high even when we consider the final values $N = 13$ cm^{-3} and $V = 11$ km s^{-1}.

Boundary Region Ions

The enhanced ion fluxes detected in all four sensors at point 7, as shown in Figure 5, were measured in the boundary region of the magnetic tail, as indicated in Figure 6. Since the amplitudes of the observed energy distributions decrease with increasing energy in all four cups, good matches of the observed distributions cannot be attained with simulations based on cycloidal distributions. This is because the cycloidal distributions are characterized by sharp decreases in the high-energy portions of the spectra simulating the D cup. On the other hand, when we simulate convective Maxwellian distributions, we obtain a good match to the data for H^+ with a bulk velocity of 40 km s^{-1} in the xy plane, which is pointed 20° to the corotational direction when the vector is rotated counterclockwise. The corresponding H^+ density is 1 cm^{-3}, and the ion temperature is 33 eV. A good match to the data is obtained for N^+ when the bulk velocity is 20 km s^{-1} in the xy plane, when the vector is rotated 40° counterclockwise from the corotational direction, the density is 22 cm^{-3} and the temperature is 29 eV. When the heavier ion N_2^+/H_2CN^+ is simulated, we find that the flow velocity must be pitched at angles as large as 50° and 60° before sufficient fluxes that match the data are obtained in the A, B, and C cups. This is not too likely unless the measurement was made, say, in the presence of a large-amplitude wave traveling along the boundary of the tail.

There is not sufficient information in the measured ion distributions to infer the ion mass. However, the ion measurement at point 7 is time coincident with the electron density of 1 cm^{-3} inferred from the plasma wave data [*Gurnett et al.*, 1981]. This density is consistent with the H^+ density inferred from the simulation of the ion distribution functions, suggesting that the H^+ at point 7 originated in Saturn's magnetosphere. In this case the ions flowing adjacent to the boundary may lose energy through collisions with the neutral atmosphere, which would reduce their bulk velocity and produce a density buildup along the flow path. The energy exchange resulting from the ion-neutral collisions should also cool these magnetospheric ions.

Magnetic Tail Plasma

The ion energy distributions measured by the D cup in Titan's magnetic tail at points 5 and 6 have narrow energy dispersions, having been observed in only two or three energy channels, as shown in Figure 5. Consequently, the velocity distributions and ion masses cannot be determined uniquely, as is the case for the cool ions of point 4. If the observed plasma flux originated in the ionosphere and flowed away from Titan along the draped field, then the distributions should approximate convective Maxwellians. In this case, simulation of the data at point 5 yields bulk speeds of 25, 5, and 3.5 km s^{-1}; densities of 1.9, 7, and 10 cm^{-3}; and temperatures of 3, 1.8, and 0.9 eV for H^+, N^+, and N_2^+/H_2CN^+, respectively. Similarily, at point 6, we obtain bulk speeds of 50, 10, and 4 km s^{-1}; densities of 1, 3, and 10 cm^{-3}; and temperatures of 3, 2.1, and 2.4 eV for H^+, N^+ and N_2^+/H_2CN^+, respectively. We note that this analysis assumes that there is no component of flow toward Titan since such flow is out of the field of view of the instrument.

These density simulations together with the electron densities of Figure 2 (outside the UV occultation region) suggest that the plasma in the tail is quite structured as a result of spatial and/or temporal variations. Variations in the ion composition are also possible. In this connection we note that the electron density in lobe L_1 of about 12 cm^{-3}, as inferred from the plasma wave measurements [*Gurnett et al.*, 1981], is closer to the N^+ and N_2^+/H_2CN^+ densities of 7 and 10 cm^{-3} than the H^+ density of 1.9 cm^{-3} at point 5, corresponding to ion measurements made about 30 s earlier.

The ion measurement at point 6 was time coincident with one of the plasma wave measurements made in lobe L_2. If the plasma waves observed at this point are due to upper-hybrid resonance emissions [*Gurnett et al.*, 1981], then the local, cold electron density lies somewhere between 4.5 and 34 cm^{-3}, based on the finite bandwidth of the plasma wave instrument [*Scarf and Gurnett*, 1977]. We note that the simulated H^+ and N^+ densities of 1 and 3 cm^{-3}, respectively, lie outside this range, while the N_2^+/H_2CN^+ density of 10 cm^{-3} lies within. Although the precise value of the mass cannot be inferred at this stage of analysis, this result suggests that light ions in the range 1 to 14 amu can be excluded at point 6, while an ion as heavy as 28 amu is possible. Since H_2CN^+ is believed to be the dominant topside ion in the ionosphere (S. K. Atreya et al., unpublished manuscript, 1981), this result is consistent with the notion of an ionospheric origin for the plasma flowing down the tail, whose principal constituent in this case would be H_2CN^+.

Electron Depletion

As noted previously, the strong decrease in the electron distribution function at energies above 700 eV was observed to occur on the draped magnetic field lines in Titan's tail. Additional electron bite-out also occurred just outside the boundary of the tail on field lines that were connected with the plasma that was slowed down by atmospheric mass loading. A likely cause of the electron depletion in the magnetic tail appears to be due to the scattering of Saturn's magnetospheric electrons by the neutral atmosphere through which the magnetic field lines thread. (A similar depletion attributed to atmospheric scattering was observed in the Venus wake by the Mariner 10 plasma science instrument—*Bridge et al.* [1974]). This can be shown by considering the change in the electron density N_e of magnetospheric electrons above 700 eV as they pass through the atmosphere along a magnetic field line. That is,

$$\cos \alpha \frac{dN_e}{dl} = -\sigma n N_e \tag{5}$$

where l is the arc length along a magnetic field line, α is the average electron pitch angle, n is the dominant neutral constituent N_2, and $\sigma \simeq 3 \times 10^{-17}$ cm^2 is a representative electron impact ionization cross section for N_2 in the energy

range 200–6000 eV. Upon integration of 5 we obtain

$$N_e = N_{0e} \exp\left(-\frac{\sigma}{\cos\alpha}\int ndl\right)$$

$$\simeq N_{0e} \exp(-\pi R\sigma n/\cos\alpha) \equiv N_{0e} \exp(-\varepsilon) \quad (6)$$

where N_{0e} is the initial electron density, ε is the extinction factor, and we assume, for simplicity, that the field line is draped over a sphere of radius R on which the density n is uniform. This expression represents the electron loss corresponding to a single electron pass through the atmosphere.

The magnetic field diffuses through the atmosphere in a time τ_D during which time an electron will mirror back and forth through the atmosphere many times. If τ_B is the bounce time for an electron on a Saturn magnetic field line, then the number of bounces N_B an electron will experience during τ_D is $N_B = \tau_D/\tau_B$. The multiple passes through the atmosphere has the effect of amplifying the density n in 6 by 2 N_B, in which case the extinction factor becomes $\varepsilon = 2\pi R\sigma n\tau_D/\tau_B \cos\alpha$. If we assume a diffusion speed $V_d \simeq 10$ km s^{-1} for a magnetic flux tube in the ionosphere, then we estimate $\tau_D = R/V_d \simeq 400$ s, when R is equal to the exobase radius. The bounce time $\tau_B \simeq 100$ s [*Schulz and Lanzerotti,* 1974] for an electron speed of 4000 km s^{-1} and a pitch angle of 45°. Using these parameters, $\varepsilon \simeq 4.2 \times 10^{-7}\, n$, which implies that the electron density will decay more than a factor of 100 when the density is greater than 10^7 cm^{-3}. This density occurs just below the ionopause, suggesting the need for an additional loss mechanism extending above the ionopause to remove those electrons on field lines just outside the magnetic tail.

Centrifugal drift produced by the centrifugal acceleration of an electron when it traverses curved magnetic field lines can be an important loss mechanism above the region where scattering is no longer important. When a magnetospheric electron moves along a field line draped around Titan, it will experience a centrifugal force $m_e V_{\|}^2/R$, where m_e is the electron mass, $V_{\|} \simeq 40{,}000$ km s^{-1} is the electron speed parallel to the magnetic field, and $R \simeq 4500$ km is the radius of curvature of the draped portion of the field in the vicinity of the ionopause. This acceleration will cause an electron to drift across the field at a speed $V_{De} = m_e V_{\|}^2/eRB \simeq 450$ km s^{-1} and a distance $\delta \simeq V_{De}(\pi R/V_{\|}) \simeq 141$ km on each pass through the Titan environment. The total distance an electron will drift after bouncing several times on a Saturn field line is $d = 2N_B\delta$. Considering that drift is important for loss in the region surrounding the subflow point, then $\tau_D \simeq R/V_d \simeq 450$ s when $V_d = 10$ km s^{-1}. This results in a total drift distance of $d \simeq 1300$ km, which is large enough to remove the electrons in the outer portions of the bite-out region since this region extends sufficiently above the altitude where collisional loss becomes unimportant.

SUMMARY

We have presented an interpretation of the ion and electron observations made close to Titan by the plasma science instrument on Voyager 1. Based upon the idea that the interaction between Titan and the rotating magnetospheric plasma of Saturn closely resembles that between Venus and the solar wind, simple models of ion pickup in the ion exosphere outside Titan's magnetic tail and ion flow within the tail have been used. The ion observations have been compared with synthetic spectra constructed from both cycloidal and Maxwellian distribution functions. The simulations take full account of the characteristics of the four Faraday cups in the plasma sensor, their directions of viewing, and spacecraft motion, and they are corrected for the background particle fluxes in the magnetosphere of Saturn and the small effects of electrons on the ion observations. Present knowledge of the atmosphere is used to estimate the minimum ionopause radius, and the neutral exosphere is represented by a spherically symmetric model composed of H and N_2.

The results of matching the observed and synthetic ion distributions indicate that the model is realistic but not unique. At points outside the tail on the side facing away from Saturn, the pickup of exospheric H^+ by the rotating magnetosphere is inferred. Also on this side of the tail, close to its boundary, a reduction in plasma flow speed is indicated, providing evidence for mass loading by the addition of N_2^+/H_2CN^+ and N^+ to the flowing plasma. One observation of the ion spectra in the boundary region of the magnetic tail on the side facing Saturn can be represented by a Maxwellian distribution, suggesting the presence of magnetospheric H^+ cooled by interaction with the neutral atmosphere. The boundary of the tail is indicated by the onset of a sharp reduction in the flux of high-energy electrons. This depletion, of 'bite-out' is due to the combined effects of inelastic scattering by Titan's neutral atmosphere and centrifugal drift as the electrons move along field lines draped around Titan. Within Titan's tail the plasma is structured as the result of spatial and/or temporal variations. Although the ion mass cannot be determined uniquely in the tail, one ion measurement, time coincident with a plasma wave measurement, suggests the presence of a heavy ion with a mass of order 28 amu. One candidate is the dominant ion of the topside ionosphere, H_2CN^+, which may flow from the ionosphere into the tail.

Acknowledgments. We wish to acknowledge H. S. Bridge's recognition of the possibility of studying plasma interaction processes with planetary atmospheres through measurements of ions picked up by flowing plasma, a capability he included in the design and configuration of the plasma science instrument. The authors also gratefully acknowledge useful comments on the interpretation of the ion observations and the manuscript by S. Olbert, J. D. Sullivan, and J. W. Belcher of MIT. N. F. Ness (GSFC) kindly allowed access to magnetic field data in advance of publication. S. Banerjee (GSFC) provided programing assistance, and F. Hunsaker and L. White (GSFC) provided support with the diagrams. S. K. Atreya acknowledges the research support received from the Planetary Atmospheres program, NASA Solar System Exploration Division.

The Editor thanks A. Eviatar and J. A. Slavin for their assistance in evaluating this paper.

REFERENCES

Atreya, S. K., T. M. Donahue, and W. R. Kuhn, Evolution of a nitrogen atmosphere on Titan, *Science, 201,* 611, 1978.

Bridge, H. S., A. J. Lazarus, J. D. Scudder, K. W. Ogilvie, R. E. Hartle, J. R. Asbridge, S. J. Bame, W. C. Feldman, and G. L. Siscoe, Observations at Venus encounter by the plasma science experiment on Mariner 10, *Science, 183,* 1293, 1974.

Bridge, H. S., J. W. Belcher, R. J. Butler, A. J. Lazarus, A. M. Mavretic, J. D. Sullivan, G. L. Siscoe, and V. M. Vasyliunas, The plasma experiment on the 1977 Voyager mission, *Space Sci. Rev., 21,* 259, 1977.

Bridge, H. S., et al., Plasma observations near Saturn: Initial results from Voyager 1, *Science, 212,* 217, 1981.

Broadfoot, A. L., el al., Extreme ultraviolet observations from Voyager 1—Encounter with Saturn, *Science, 212,* 206, 1981.

Gurnett, D. A., W. S. Kurth, F. L. Scarf, Plasma waves near Saturn: Initial results from Voyager 1, *Science, 212,* 235, 1981.

Hanel, R., et al., Infrared observations of the Saturnian system from Voyager 1, *Science, 212,* 192, 1981.

Hartle, R. E., Model for rotating and nonuniform planetary exospheres, *Phys. Fluids, 14,* 2592, 1971.

Hartle, R. E., H. A. Taylor, Jr., S. J. Bauer, L. H. Brace, C. T. Russell, and R. E. Daniell, Jr., Dynamical response of the dayside ionosphere of Venus to the solar wind, *J. Geophys. Res., 85,* 7739, 1980.

Hunten, D. M., Titan's atmosphere and surface, in *Planetary Satellites*, edited by J. A. Burns, p. 420, University of Arizona Press, Tucson, 1977.

Kuiper, G. P., Titan: A satellite with an atmosphere, *Astrophys. J., 100,* 378, 1944.

Michel, F. C., Solar-wind-induced mass loss from magnetic field-free planets, *Planet. Space Sci., 19,* 1580, 1971.

Ness, N. F., M. H. Acuna, R. P. Lepping, J. E. P. Connerney, K. W. Behannon, L. F. Burlaga, F. M. Neubauer, Magnetic field studies by Voyager 1: Preliminary results at Saturn, *Science, 212,* 211, 1981.

Russell, C. T., R. C. Elphic, and J. A. Slavin, Limits on possible intrinsic magnetic field of Venus, *J. Geophys. Res., 85,* 8319, 1980.

Scarf, F. L., and D. A. Gurnett, Plasma wave investigation for the Voyager mission, *Space Sci. Rev., 21,* 289, 1977.

Schulz, M., and L. J. Lanzerotti, *Particle Diffusion in the Radiation Belts,* Springer, New York, 1974.

Scudder, J. D., E. C. Sittler, Jr., and H. S. Bridge, Survey of the plasma electron environment of Jupiter: A view from Voyager, *J. Geophys. Res., 86,* 8157, 1981.

Sittler, E. C., Jr., J. D. Scudder, and H. S. Bridge, Distribution of neutral gas and dust near Saturn, *Nature, 292,* 711, 1981.

Tyler, G. L., V. R. Eshleman, J. D. Anderson, G. S. Levy, G. F. Lindal, G. E. Wood, T. A. Croft, Radio science investigations of the Saturn system with Voyager 1: Preliminary results, *Science, 212,* 201, 1981.

Vasyliunas, V. M., Deep-space plasma measurements, in *Methods of Experimental Physics*, vol. 9B, *Plasma Physics*, edited by R. H. Lovberg, p. 49, Academic, New York, 1971.

Wallis, M. K., Weakly-shocked flows of the solar wind plasma through atmospheres of comets and planets, *Planet. Space Sci., 21,* 1647, 1973.

(Received July 31, 1981;
revised September 30, 1981;
accepted October 2, 1981.)